Electronic Supplementary Information (ESI)

Ultrafast removal of organics via peroxymonosulfate activation over Co_2P/TD hollow spheres derived from ZIF-67

Fei Wang, Yu-Hang Li, Ya Gao, Yutong Chai, Yuwei Wei, Chong-Chen Wang,* Peng Wang, Huifen Fu, and Chen Zhao

Beijing Key Laboratory of Functional Materials for Building Structure and Environment Remediation, School of Environment and Energy Engineering, Beijing University of Civil Engineering and Architecture, Beijing 100044, China

Chemical and reagents

Cobaltous nitrate hexahydrate ($Co(NO_3)_2·6H_2O$, 98%), potassium peroxomonosulfate (PMS, 4.5% active oxygen), *tert*-Butanol (TBA, 99.5%), 4-Hydroxybenzoic acid (HBA, 99%), β-Carotene (97%), phenol (PN, 98%), bisphenol A (BPA, 96%), tetracycline (TTC, 91%), sulfamethoxazole (SMX, 98%) were purchased from J&K Scientific Company. 2-Methylimidazole (2-MIN, 98%) was purchased from JIANGSU B-WIN CHEMICAL CO., LTD. Sodium phytate (SPT, 97%) was obtained from ShanghaiShaoyuan Co., Ltd. Ofloxacin (OFC, 98%), benzoquinone (BQ, 98%), benzoic acid (BA, 98%), 4-Nitrobenzoic acid (4-NP, 98%), nitro-blue tetrazolium (NBT, 98%) were purchased from Shanghai Macklin Biochemical Co., Ltd. Ammonium Bicarbonate (NH_4HCO_3, 99%), sodium chloride (NaCl, 99%), sodium sulfate (Na_2SO_4, 99%), sodium nitrate ($NaNO_3$, 99%), sodium dihydrogen phosphate (NaH_2PO_4, 99%), sulfuric acid (H_2SO_4), sodium hydroxide (NaOH), rhodamine B (RhB, 98%) were provided by Sinopharm Chemical Reagent Co., Ltd. $_L$-Histidine (98%) was purchased from TOKYO CHEMICAL INDUSTRY Co., Ltd. Ethanol absolute (99.5%), methanol (99.8%) were obtained from Fuchen (Tianjin) Chemical Reagent Co., Ltd.

Synthesis of catalysts

ZIF-67: $Co(NO_3)_2·6H_2O$ (2 mmol, 582 mg) and 2-MI (8 mmol, 656 mg) were dissolved in 7.5 mL methanol, respectively and ultrasonic treatment for 10 min. Then the two solutions were mixed and put into a Teflon-lined autoclave (100 mL) to be heated at 120 °C for 2 h. The generated products were washed three times with methanol and dried at 60 °C overnight.

ZIF-67/SPT-x: x (x = 50, 100, and 150, representing the mass of ZIF-67) mg of as-synthesized ZIF-67 and 1.0 g of sodium phytate (SPT) were dissolved in 50 mL of methanol. Then the mixed solution was stirred on a magnetic stirrer at 80 °C until the methanol solution was evaporated to dryness. Finally, the ZIF-67/SPT-x catalysts were successfully prepared.

Co_2P/TD-x: The as-synthesized ZIF-67/SPT-x catalysts were transferred into a tube furnace and heated at 800 °C with the heating rate of 5 °C/min for 2 h under N_2 atmosphere (Fig. S1). After cooling to room temperature, the Co_2P/TD-x catalysts were obtained. For comparison, the individual Co-N/C catalyst was synthesized without the addition of SPT.

Characterization techniques

Powder X-ray diffraction (PXRD) patterns were recorded on a Dandonghaoyuan DX-2700B diffractometer in the range of 2ϑ = 5°-50° with Cu K_α radiation. The morphology of the materials was observed by scanning electron microscopy (SEM) (SU8020, Hitachi Limited, Japan). X-ray photoelectron spectroscopy (XPS) was measured using a Thermo ESCALAB 250XI. The content of elements of Co of as-prepared catalysts were detected by inductively coupled plasma optical emission spectrometer (ICP-OES). Electron spin resonance (ESR) spectra were obtained by a JEOL JES-FA200 instrument using 5,5-dimethyl-1-pyrroline-N-oxide (DMPO) and 2,2,6,6-Tetramethylpiperidine (TEMP) as spin-trapping agents to detect $SO_4^{\bullet-}$, $^{\bullet}OH$, $O_2^{\bullet-}$ and $^1O_2$. EIS and LSV curves were obtained by Metrohm Autolab PGSTAT204 electrochemical station using a typical three-electrode mode in 0.2 M Na_2SO_4 aqueous solution.

Quantification of $SO_4^{\bullet-}$, $^{\bullet}OH$, and $^1O_2$.

The generated $SO_4^{\bullet-}$ in the Co_2P/TD-50/PMS/PN system was quantified by detecting 4-benzoquinone (BQ) that was produced from the reaction of p–hydroxybenzoic acid (HBA) and $SO_4^{\bullet-}$. Typically, a specific molar ratio of HBA and PMS were added into 50.0 mL of deionized water, in which Co_2P/TD-50

was added as SR-AOP catalyst. At pre-set time interval, 1.5 mL of sample was taken out and filtered by 0.22 μm PTFE filter. Meanwhile, the excessive methanol (10.0 μL) was immediately added to quench ROSs. The optimal molar ratio of HBA:PMS was 6:1. The formed BQ, as a stable byproduct, can be detected by UHPLC, in which the wavelength of the UV detector was set as 246 nm. Finally, the $SO_4^{\bullet-}$ concentrations were calculated based on the stoichiometric ratio of $SO_4^{\bullet-}$ to BQ.[1]

The generated $^{\bullet}OH$ in the Co_2P/TD-50/PMS/PN system was quantified by detecting p–hydroxybenzoic acid (HBA) that was produced from the reaction of benzoic acid (BA) and $^{\bullet}OH$. The specific process was similarly to the Quantification of $SO_4^{\bullet-}$. The optimal molar ratio of BA:PMS was 4:1. The generated HBA could be detected by UHPLC, in which the wavelength of the UV detector was set as 254 nm. Finally, Cumulative $^{\bullet}OH$ concentration was estimated from 5.87 times of HBA concentration.[2]

The 1,3-diphenylisobenzofuran (DPBF) (0.2 mol/L, λ = 410 nm) was used as a trapping agent to quantify singlet oxygen ($^1O_2$). The concentration of $^1O_2$ was obtained by the consumed DPBF due to their stoichiometric ratio was 1:1.[3]

The steady-state concentrations of $SO_4^{\bullet-}$, and $^{\bullet}OH$ in the Co_2P/TD-50/PMS/PN system

The NBA, and BA were applied as probes to calculate the steady-state concentrations of $SO_4^{\bullet-}$, and $^{\bullet}OH$ in the Co_2P/TD-50/PMS system,[4,5] and the NBA, and BA degradation in the Co_2P/TD-50/PMS system exhibited as follows:

$$\frac{d[NBA]}{dt} = -k_{NBA,\bullet OH}[^{\bullet}OH]_{ss}[NBA] \quad (S1)$$

$$\frac{d[BA]}{dt} = -(k_{BA,\bullet OH}[^{\bullet}OH]_{ss}[BA] + k_{BA,SO4\bullet^-}[SO_4^{\bullet-}]_{ss})[BA] \quad (S2)$$

Integrating Eqs. S1–S2 could yield:

$$\ln\frac{[NBA]}{NBA_0} = -k_{NBA,\bullet OH}[^{\bullet}OH]_{ss}t = -k_{NBA}t \quad (S3)$$

$$\ln\frac{[BA]}{BA_0} = -(k_{BA,\bullet OH}[^{\bullet}OH]_{ss}t + k_{BA,SO4\bullet^-}[SO_4^{\bullet-}]_{ss})t = -k_{BA}t \quad (S4)$$

Then, $[^{\bullet}OH]_{ss}$, and $[SO_4^{\bullet-}]_{ss}$ could be obtained:

$$[^{\bullet}OH]_{ss} = \frac{k_{NBA}}{k_{NBA,\bullet OH}} \quad (S5)$$

$$[SO_4^{\bullet-}]_{ss} = \frac{k_{BA} - k_{BA,\bullet OH} \times [\bullet OH]ss}{k_{SO_4^{\bullet-},BA}} \quad (S6)$$

Where, [NBA], and [BA] represent the concentrations of NBA, and BA at a specific time, respectively; $[NBA]_0$, and $[BA]_0$ are the initial concentrations of NBA, and BA, respectively; $k_{NBA,HO\bullet}$ is the second-order rate constant of NBA with $HO^{\bullet}$ (2.6×10^9 $M^{-1}s^{-1}$); $k_{BA,HO\bullet}$ and $k_{BA,SO4\bullet-}$ is the second-order rate constant of BA with $HO^{\bullet}$ (2.1×10^9 $M^{-1}s^{-1}$) and $SO_4^{\bullet-}$ (1.2×10^9 $M^{-1}s^{-1}$), respectively; $[HO^{\bullet}]_{ss}$, and $[SO_4^{\bullet-}]_{ss}$ refer to the steady-state concentrations of $HO^{\bullet}$, and $SO_4^{\bullet-}$, respectively. The pseudo-first- order rate constants of NBA (k_{NBA}), and BA (k_{BA}) can be obtained from the plots of $-\ln([NBA]/[NBA]_0)$, and $-\ln([BA]/[BA]_0)$ versus time, respectively.

The contribution of $SO_4^{\bullet-}$, $^{\bullet}OH$, and $^1O_2$ for PN degradation in the Co_2P/TD-50/PMS system

After the steady–state concentrations of $SO_4^{\bullet-}$, and $^{\bullet}OH$ were calculated, the contributions of $SO_4^{\bullet-}$, $^{\bullet}OH$, and $^1O_2$ to PN degradation were calculated as follows:

$$R^{\bullet}OH = \frac{k_{PN,\bullet OH} \times [\bullet OH]ss}{k_{PN}} \quad (S7)$$

$$RSO_4^{\bullet-} = \frac{k_{PN,SO_4\bullet^-} \times [SO_4\bullet^-]ss}{k_{PN}} \quad (S8)$$

$$R^1O_2 = 1\text{-}R^{\bullet}OH - RSO_4^{\bullet-} \quad (S9)$$

Where, $k_{PN,HO\bullet}$, and $k_{PN,SO4\bullet-}$ are the second–order rate constant of PN with $^{\bullet}OH$ (5.1×10^9 $M^{-1}s^{-1}$), and $SO_4^{\bullet-}$ (4.3×10^9 $M^{-1}s^{-1}$), respectively; k_{PN} is the pseudo-first-order rate constant of PN; $R_{HO\bullet}$, $R_{SO4\bullet-}$, and $R^1{}_{O2}$ are the relative contribution of $^{\bullet}OH$, $SO_4^{\bullet-}$, and $^1O_2$, respectively.

SR-AOP catalytic performance tests

All batch experiments were conducted in the dark. The initial concentrations of PN, CQ, TTC, SMX, OFC, and RhB were 10.0 mg/L. All catalytic degradation experiments for PMS activation were conducted in a PCX-50C reactor (Beijing Perfectlight Technology Co., Ltd.). Typically, 0.1 g/L of catalyst and 0.4 mM of PMS were added to 50.0 mL of PN solution to initiate the degradation reaction. At specific time intervals, 1.0 mL of reaction solution was extracted, immediately filtered, and quenched with 15.0 μL of methanol. Finally, the residue concentration of PN was detected by the High-performance liquid chromatography (HPLC, Thermo Scientific Vanquish Flex).

Fabrication of Co_2P/TD-50/PVDF membrane

100.0 mg of Co_2P/TD-50 was dispersed into 50.0 mL of ultrapure water with ultrasound to form a suspension, which was deposited on a PVDF filter membrane with the surface area of 19.625 cm^2 (pore size = 0.45 μm) via a direct vacuum-assisted filtration of Co_2P/TD-50 suspensions.

SR-AOP catalytic performance of continuous-flow operation

The continuous-flow catalytic degradation of PN was conducted via the Co_2P/TD-50/PVDF fixed membrane reactor. A peristaltic pump (BT100-1F) with a flow rate of 7.5 mL/min and a microinject pump (LD-P2020) with a flow rate of 0.4 mL/h were applied to deliver the PN (10.0 mg/L) and PMS (250.0 mM) solutions, respectively.

Table S1 The concentration of Co element in different catalysts

Catalysts	ICP-OES (ωt %)
Co_2P/TD-25	0.7214
Co_2P/TD-50	1.6738
Co_2P/TD-100	4.2436

Table S2 Textural properties of Co_2P/TD-x

Catalysts	Surface Area (m^2/g)	Average Pore Size (nm)
Co_2P/TD-25	4.1	4.48
Co_2P/TD-50	74.4	6.89
Co_2P/TD-100	43.1	3.08

Table S3 Comparison of different catalysts for PN degradation via PMS activation

Catalysts (g/L)	Organics (mg/L)	PMS dosage (mM)	Degradation efficiency (%)	Time (min)	Ref.
Co@ACFA-BC (0.1)	PN (50)	1.0	100	60	[6]
8-g C_3N_4/Mo/Ni (0.25)	PN (20)	0.5	98	60	[7]
FeCo-DAC (0.2)	PN (20)	0.4	100	4	[8]
N–doped CNS (0.1)	PN (20)	3.25	97	120	[9]
C–Mn (0.4)	PN (30)	1.7	100	90	[10]
CPANI–9 (0.025)	PN (1)	0.5	100	10	[11]
NoCNT–700 (0.1)	PN (20)	0.5	100	20	[12]
Co_3O_4–rGO (0.07)	PN (20)	3.4	100	20	[13]
FeCo–N/C (0.05)	PN (15.3)	1.3	100	20	[14]
Co_2P/TD-50 (0.1)	PN (10)	0.4	100	4	This work

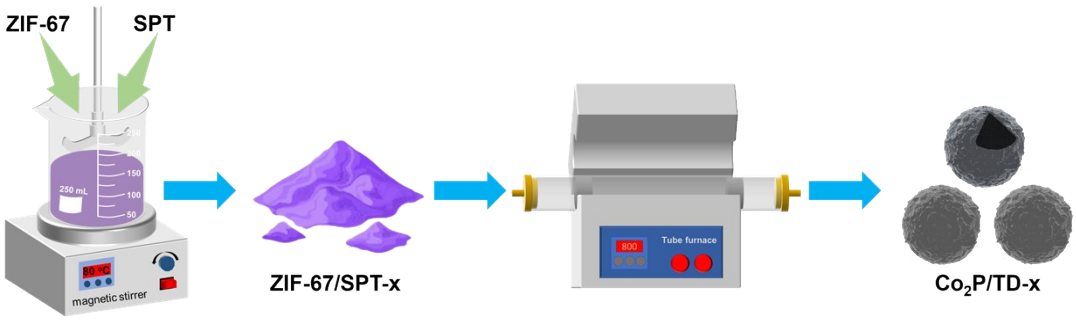

Fig. S1 The synthesis process of Co_2P/TD-x.

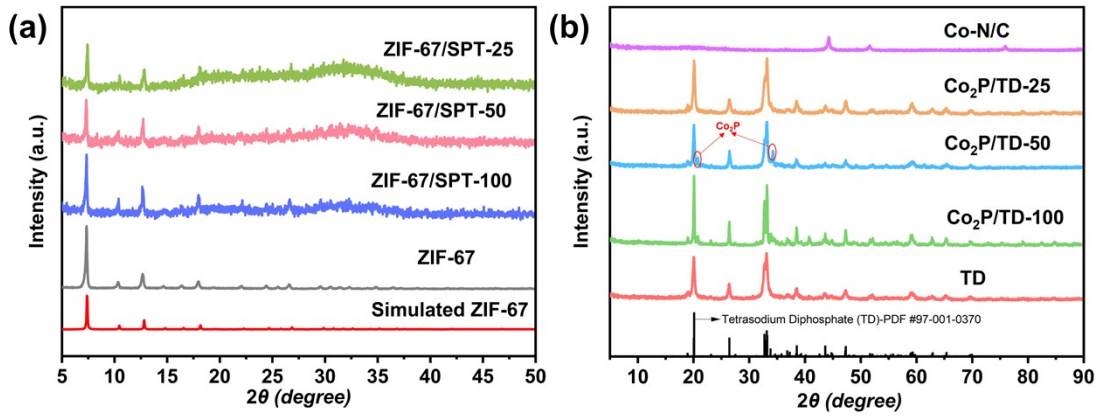

Fig. S2 PXRD patterns of (a) ZIF-67, simulated ZIF-67, ZIF-67/SPT-x, and (b) Co-N/C, Co_2P/TD-x, and TD.

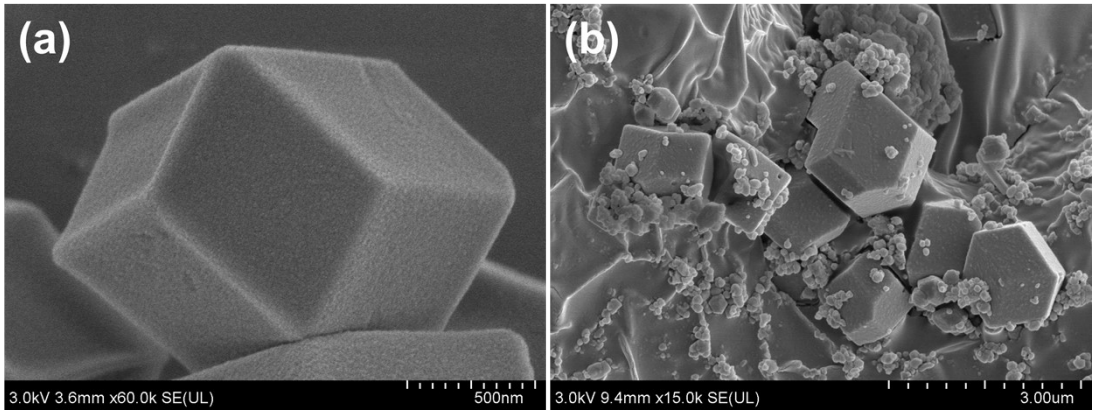

Fig. S3 SEM images of (a) ZIF-67 and (b) ZIF-67/SPT-50.

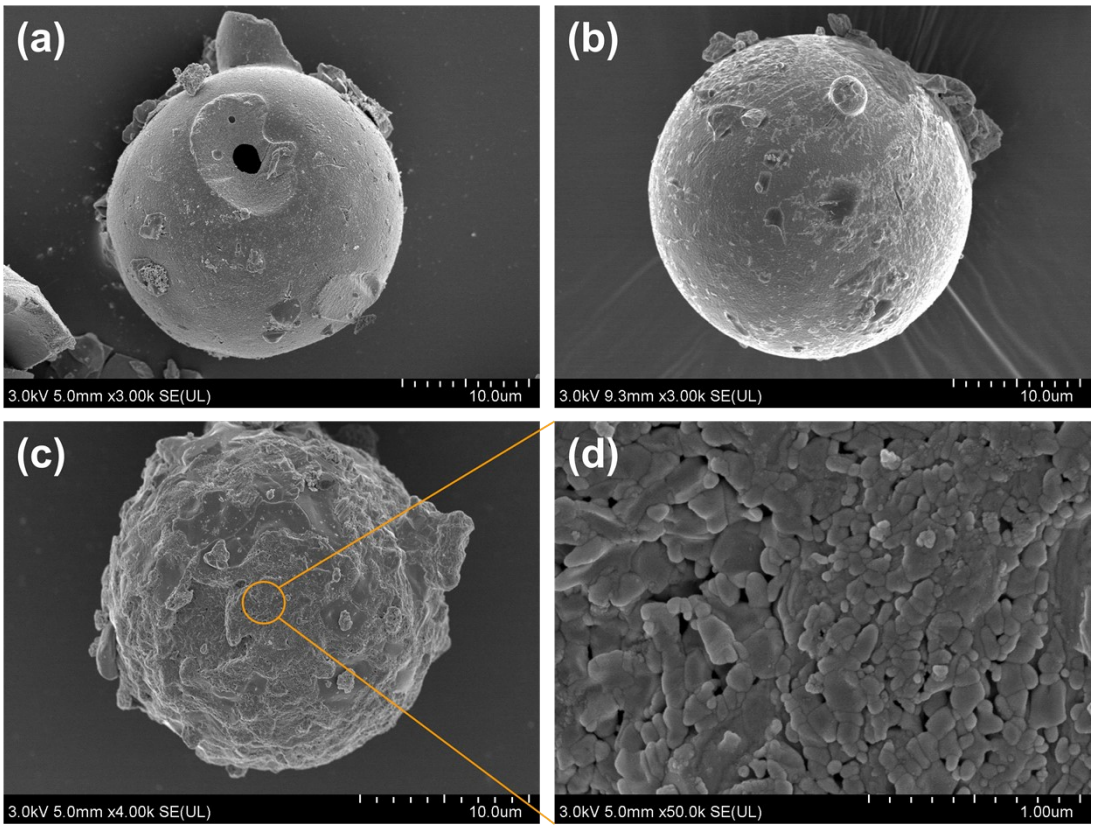

Fig. S4 SEM images of (a-b) individual TD derived from SPT and (c-d) Co_2P/TD-50.

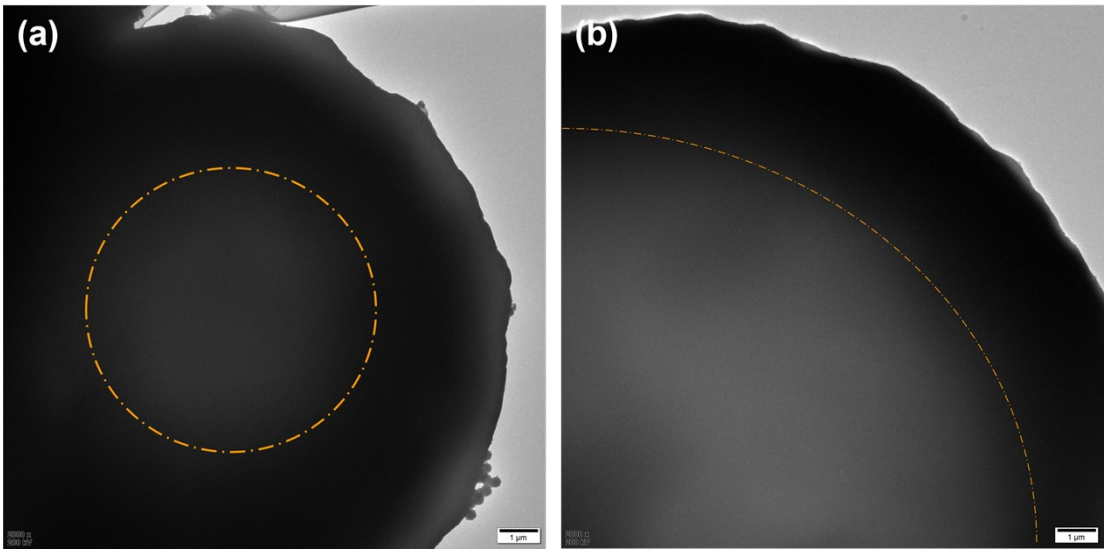

Fig. S5 (a-b) TEM images of Co_2P/TD-50.

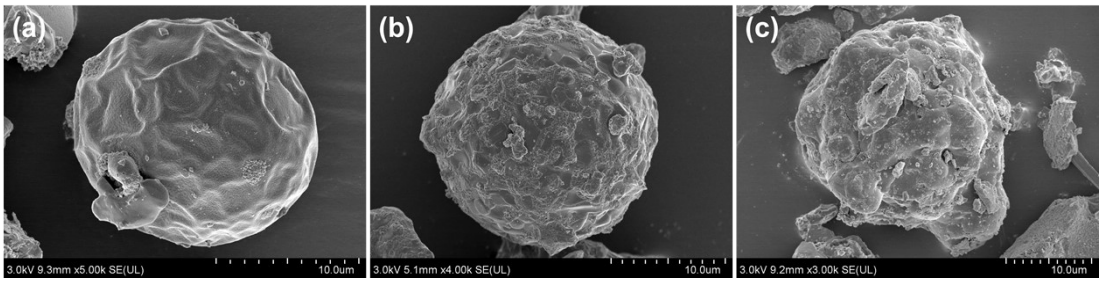

Fig. S6 SEM images of (a) Co_2P/TD-25, (b) Co_2P/TD-50, and (c) Co_2P/TD-100.

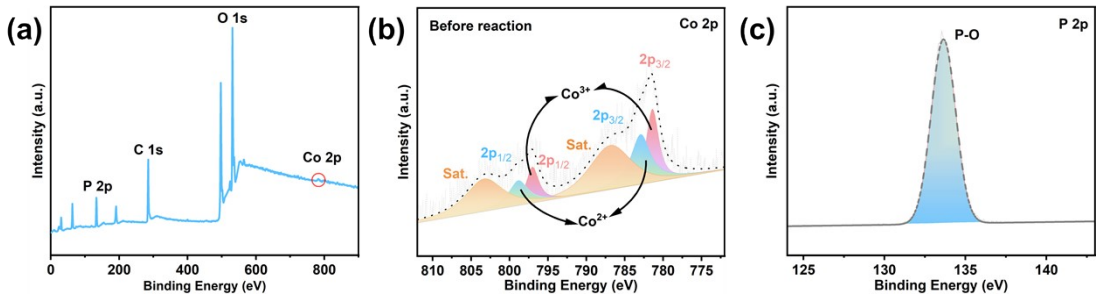

Fig. S7 (a) XPS survey spectra and high-resolution XPS spectra of (b) Co 2p, and (c) P 2p.

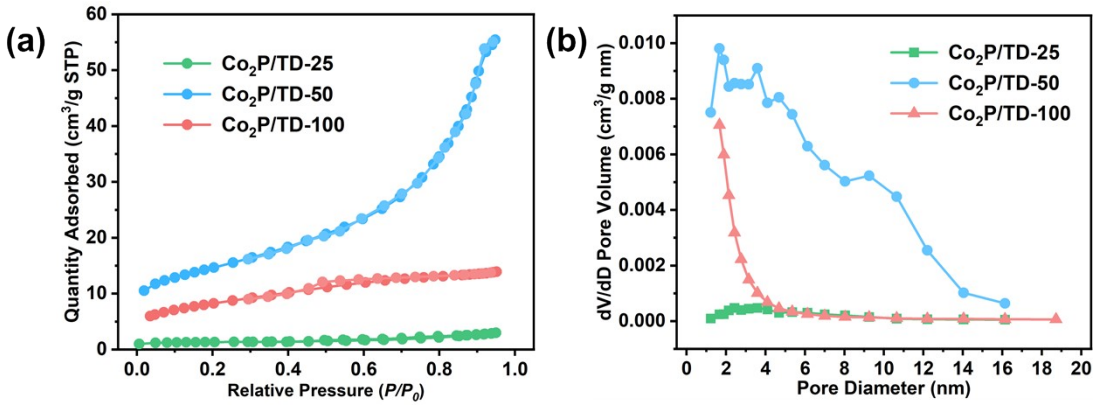

Fig. S8 (a) The N_2 adsorption–desorption isotherm and (b) pore size distribution of Co_2P/TD-x.

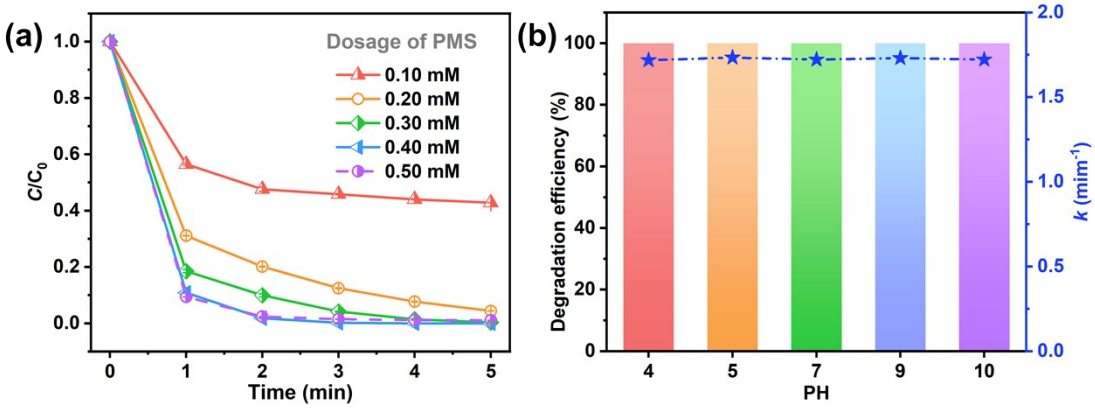

Fig. S9 Influences of (a) PMS dosage and (b) initial pH on PN degradation.

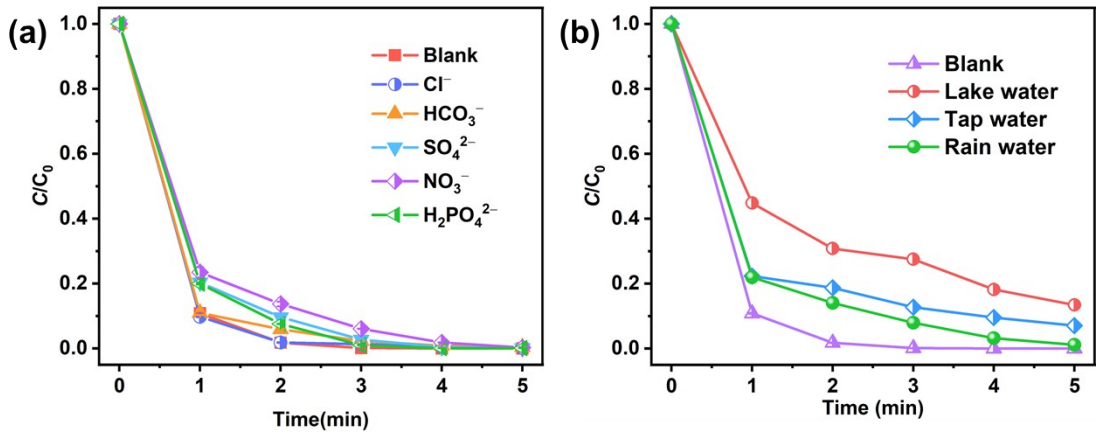

Fig. S10 Influences of (a) inorganic anions and (b) different simulated waterbody on PN degradation.

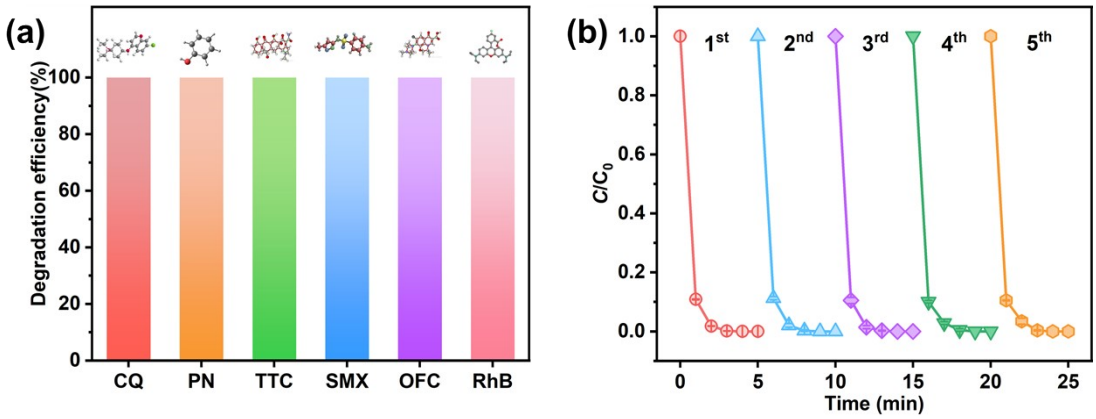

Fig. S11 (a) Removal of multiple pollutants by Co_2P/TD-50 catalyst and structures of the relevant pollutants (inset) and (b) cycling experiments of PN degradation over Co_2P/TD-50.

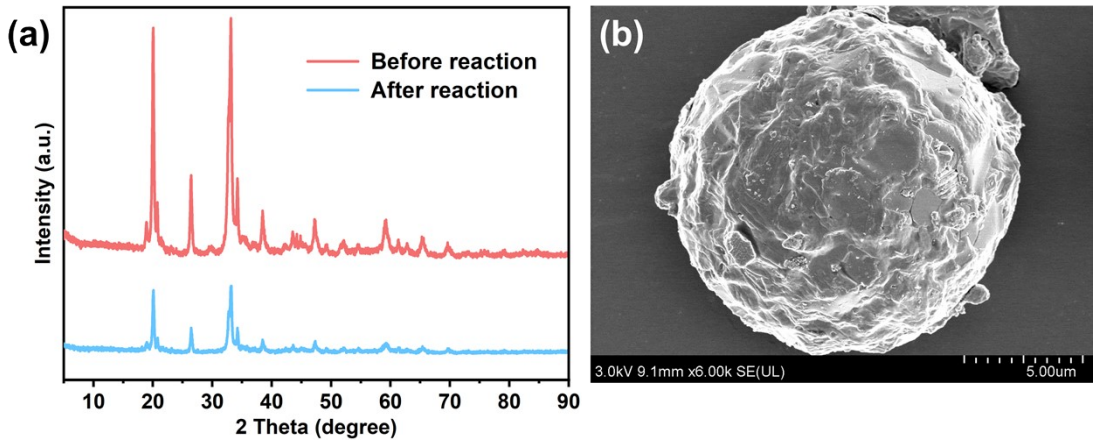

Fig. S12 (a) PXRD pattern and (b) SEM image of Co_2P/TD-50 after reaction.

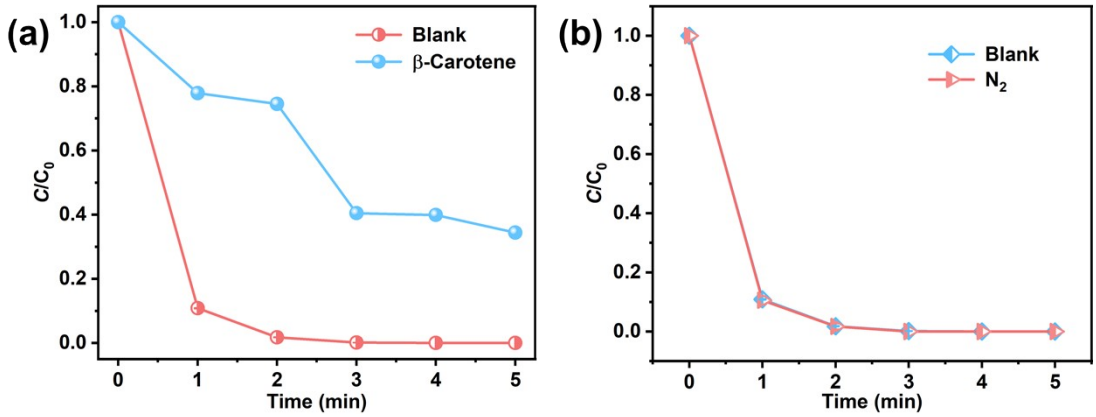

Fig. S13 Influences of (a) β-Carotene and (b) N_2 on PN degradation.

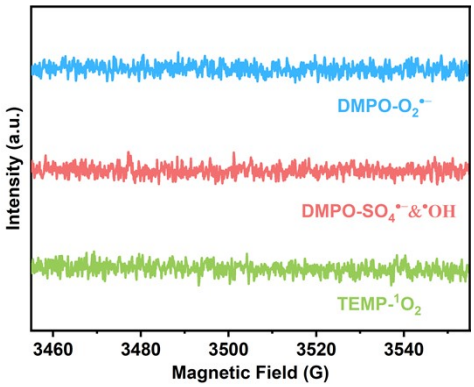

Fig. S14 ESR spectrum of DMPO-$SO_4^{\bullet-}$&•OH, DMPO-$O_2^{\bullet-}$, and TEMP-$^1O_2$ in the individual PMS system.

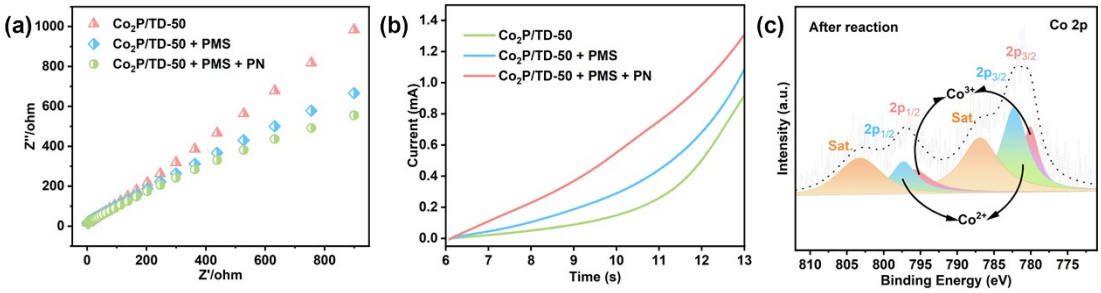

Fig. S15 (a) Electrochemical impedance spectroscopy (EIS), (b) Linear sweep voltammetry (LSV) in different systems, and (c) Co 2p XPS spectra after reaction of Co_2P/TD-50.

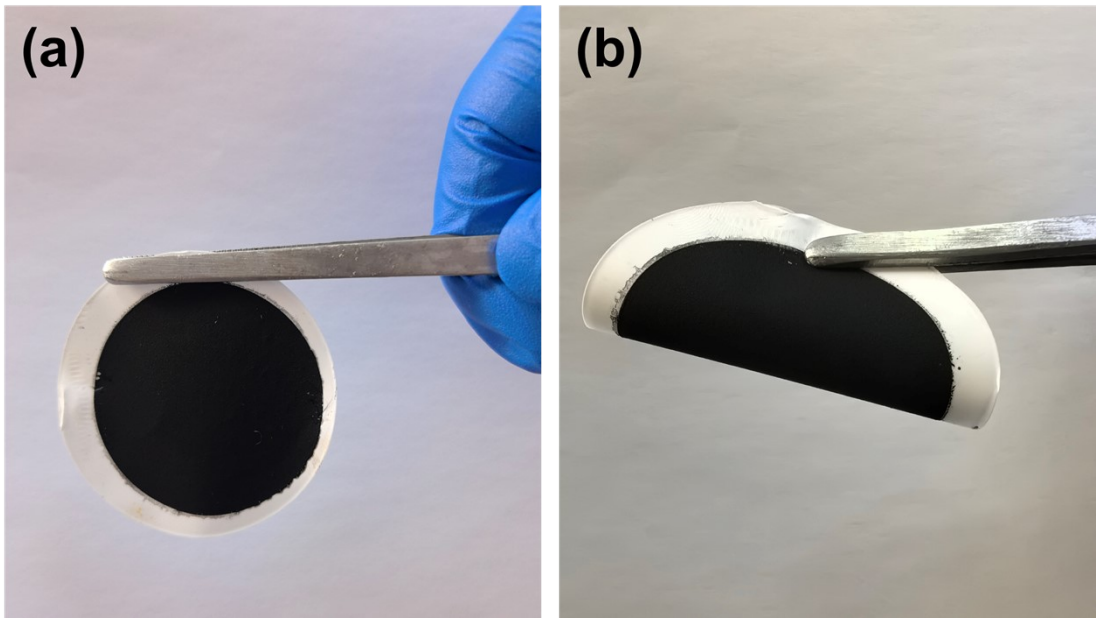

Fig. S16 (a-b) photograph of as-prepared Co_2P/TD-50/PVDF membrane.

Notes and references

1. F. Wang, H. Fu, F.-X. Wang, X.-W. Zhang, P. Wang, C. Zhao and C.-C. Wang, *J. Hazard Mater.*, 2022, **423**, 126998.
2. N. Chen, D. Huang, G. Liu, L. Chu, G. Fang, C. Zhu, D. Zhou and J. Gao, *Water Res.*, 2021, **203**, 117484.
3. Z.-C. Zhang, F.-X. Wang, F. Wang, C.-C. Wang and P. Wang, *Sep. Purif. Technol.*, 2023, **307**, 122864.
4. F. Wang, Y. Gao, H. Chu, Y. Wei, C.-C. Wang, S.-S. Liu, G. Liu, H. Fu, P. Wang and C. Zhao, *ACS ES&T Engg.*, 2024, **4**, 153-165.
5. M. Yang, Z. Hou, X. Zhang, B. Gao, Y. Li, Y. Shang, Q. Yue, X. Duan and X. Xu, *Environ. Sci. Technol.*, 2022, **56**, 11635-11645.
6. F. Meng, Y. Wang and Q. Cao, *Chemosphere*, 2023, **337**, 139441.
7. M. Tian, X. Ren, S. Ding, N. Fu, Y. Wei, Z. Yang and X. Yao, *Environ. Res.*, 2024, **243**, 117848.
8. F. Wang, Y. Gao, H. Fu, S.-S. Liu, Y. Wei, P. Wang, C. Zhao, J.-F. Wang and C.-C. Wang, *Appl. Catal. B: Environ.*, 2023, **339**, 123178.
9. P. Hu, H. Su, Z. Chen, C. Yu, Q. Li, B. Zhou, P. J. J. Alvarez and M. Long, *Environ. Sci. Technol.*, 2017, **51**, 11288-11296.
10. N. Tian, X. Tian, Y. Nie, C. Yang, Z. Zhou and Y. Li, *Chem. Eng. J.*, 2018, **352**, 469-476.
11. S. Liu, Z. Zhang, F. Huang, Y. Liu, L. Feng, J. Jiang, L. Zhang, F. Qi and C. Liu, *Appl. Catal. B: Environ.*, 2021, **286**, 119921.
12. X. Duan, H. Sun, Y. Wang, J. Kang and S. Wang, *ACS Catal.*, 2015, **5**, 553-559.
13. Y. Yao, Z. Yang, H. Sun and S. Wang, *Industrial & Engineering Chemistry Research*, 2012, **51**, 14958-14965.
14. Z. Zhao, W. Zhou, D. Lin, L. Zhu, B. Xing and Z. Liu, *Appl. Catal. B: Environ.*, 2022, **309**, 121256.